



REVIEW

Nanomaterials for renewable hydrogen production, storage and utilization

Samuel S. Mao^{a,*}, Shaohua Shen^{a,b}, Liejin Guo^b

^aLawrence Berkeley National Laboratory and Department of Mechanical Engineering, University of California at Berkeley, Berkeley, CA 94720, United States

^bInternational Research Center for Renewable Energy, State Key Laboratory of Multiphase Flow in Power Engineering, Xi'an Jiaotong University, Shaanxi 710049, China

Received 23 August 2012; accepted 10 November 2012

Available online 10 January 2013

KEYWORDS

Nanomaterials;
Renewable energy;
Hydrogen production;
Fuel cell;
Hydrogen storage

Abstract An ever growing demand for energy coupled with increasing pollution is forcing us to seek environmentally clean alternative energy resources to substitute fossil fuels. The rapid development of nanomaterials has opened up new avenues for the conversion and utilization of renewable energy. This article reviews nanostructured materials designed for selected applications in renewable energy conversion and utilization. The review is based on the authors' research, with particular focus on solar hydrogen production, hydrogen storage and hydrogen utilization. The topics include photoelectrochemical (PEC) water splitting and photocatalytic hydrogen production, solid-state hydrogen storage, and proton exchange membrane fuel cells (PEMFCs). It is expected that the rational design of nanomaterials could play an important role in achieving a renewable energy based economy in the coming decades.

© 2012 Chinese Materials Research Society. Production and hosting by Elsevier B.V. All rights reserved.

1. Introduction

As the global consumption of fossil fuels grows at an alarming and unsustainable rate, the associated emissions of greenhouse gases and other toxic pollutants are reaching levels that are environmentally unacceptable. The future sustainable development of society

relies on alternative energy sources that are renewable and environmentally friendly. As the sun is our largest and cheapest (free) energy resource available, it could be considered the ultimate renewable energy resource. It continuously bombards our planet with solar energy, with 1 h of solar energy equating to more than all of our annual energy consumption [1]. Among the limited

*Corresponding author.

E-mail address: ssmao@lbl.gov (S.S. Mao).

Peer review under responsibility of Chinese Materials Research Society.



Production and hosting by Elsevier

methods for solar energy conversion and utilization, solar water splitting has been considered as the most effective and cleanest way to produce hydrogen. The hydrogen produced can then be used by fuel cells to generate electricity, where water constitutes the only emission. Starting from solar energy conversion and ending with hydrogen utilization, a renewable energy based economy could be proposed and successfully structured in the coming decades. Fig. 1 shows the scheme of a renewable energy economy (e.g., solar energy and hydrogen) based on some selected technologies of renewable energy conversion and utilization. In order for solar energy to be the major contributor to the generation of clean fuel (hydrogen), the efficiencies of solar water-splitting devices need to be improved. Technologies for high-capacity hydrogen-storage and high performance fuel cells must also be developed in order for hydrogen to become the primary fuel for future renewable energy based economy [2].

Throughout human history, advances in civilization have been associated with the discovery, development, and use of new materials [3]. In many respects, materials can be considered as the parents of almost all technologies as most technological breakthroughs have been achieved through the development of new materials. Nanomaterials are beginning to play an important role in creating new fields of science and new nanotechnologies. In order to achieve technological breakthroughs in effective renewable energy conversion, storage, and utilization, we need smart nanomaterials to fully develop the potential of renewable energy. To this end, the potential capabilities of nanomaterials must be extensively discovered at a more fundamental level.

In this article, we provide a brief overview on nanomaterial designs for selected technologies of renewable energy conversion and utilization, based on the research activities of the Clean Energy Engineering Laboratory in the University of California at Berkeley. The topics include (1) photoelectrochemical (PEC) water splitting, (2) photocatalytic hydrogen production, (3) solid-state hydrogen storage, and (4) proton exchange membrane fuel cells (PEMFCs). We hope that these concepts of nanomaterial designs will offer a new paradigm for realizing a renewable energy based economy in the not so distant future.

2. Nanostructured electrodes for PEC water splitting

Pioneered by Fujishima and Honda, the first reported success on solar-driven water splitting in a photoelectrochemical (PEC) cell

consisted of a TiO_2 anode and Pt cathode for oxygen and hydrogen production [4]. PEC water splitting has been considered as the most attractive method over other hydrogen production approaches. As schematically shown in Fig. 2, when a TiO_2 anode is irradiated by light with energy larger than its band gap, electrons and holes are generated in the conduction and valence bands, respectively [5]. As a result, water is oxidized by photo-generated holes on the TiO_2 anode to produce oxygen, while photogenerated electrons transfer to the Pt counter electrode and participate in hydrogen production. In the PEC process, oxygen production on photoanodes, involved in a 4-electron reaction, is kinetically limited for water splitting. Thus, much research effort has been focused on the design of nanostructured photoanodes for oxygen production via PEC water splitting.

TiO_2 represents one of the most important semiconductor materials for PEC water splitting [6,7]. Due to its large band gap of about 3.2 eV, TiO_2 cannot absorb visible and infrared light for solar water splitting. Thus, doping of either metal or non-metal ions has been widely adopted to narrow the band gap of TiO_2 by introducing acceptor or donor levels in the forbidden band, making TiO_2 sensitive to visible light [5,6]. For example, a C-doped TiO_2 nanocrystalline film, prepared by controlled combustion of Ti metal in a natural gas flame, exhibited a high water-splitting performance with a total conversion efficiency of

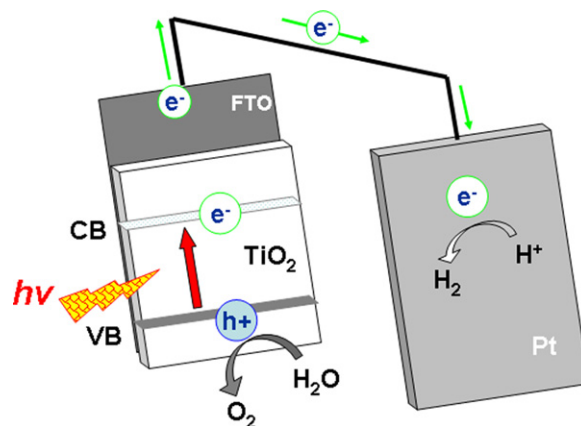


Fig. 2 Schematic representation of a photoelectrochemical (PEC) cell.

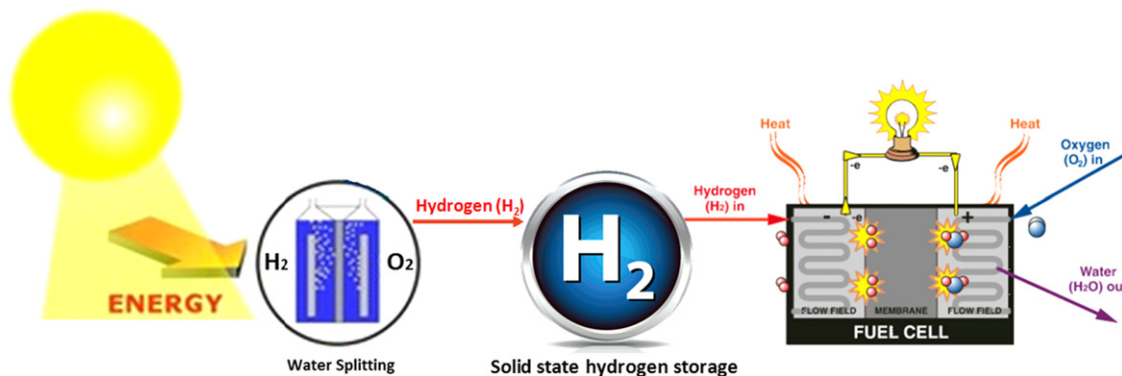


Fig. 1 A scheme of renewable energy (e.g., solar energy and hydrogen) based economy based on some selected technologies of renewable energy conversion and utilization.

11% and a maximum photoconversion efficiency of 8.35%. This was mainly due to its enhanced visible light absorption [8]. The morphology of TiO_2 anodes will also affect the PEC water splitting performance, by varying the charge transfer ability. Grimes and co-workers prepared and examined the use of TiO_2 nanotube arrays for PEC water splitting, which greatly benefits from the nanotubular architecture that gave rise to superior electron lifetimes and, hence, more efficient charge separation [9–15]. A high photoconversion efficiency of 16.5% under UV light illumination could be obtained with 24 μm -long nanotubes electrochemically fabricated in an ethylene glycol based electrolyte [14].

The electron transfer process, considered as an interfacial phenomenon greatly determining the performances of various (opto)electronic devices, including solar cells and PEC water splitting cells, is directly influenced by the character and occupancy of electronic states near the interface. Thus, our group investigated the electronic structure of the interface of TiO_2 and fluorine-doped tin dioxide ($\text{SnO}_2\text{:F}$, and FTO), one of the most common transparent conductive oxides (TCO) used as substrates for photoelectrodes in PEC cells, by a synchrotron-based soft x-ray absorption spectroscopy (XAS) [16]. The distinct interfacial electronic structure of $\text{TiO}_2\text{-SnO}_2\text{:F}$ was established by contrasting spectra with those for anatase and rutile TiO_2 , $\text{SnO}_2\text{:F}$, and $\text{ZnO-SnO}_2\text{:F}$ and $\text{CdO-SnO}_2\text{:F}$ interfaces. Oxygen 1s absorption spectra, as shown in Fig. 3 and which relate to the O 2p partial density of states of the conduction band, indicated that the interface was associated with a reduction in Ti $d\text{-O } p$ orbital hybridization and an alteration of the TiO_2 crystal field. These observations were consistent with measured Ti 2p absorption spectra (Fig. 4), which in addition provided an evidence for the distortion of long-range order around the cation site in the interfacial TiO_2 . The results indicate that the quasi-Fermi level of electrons in the interface will differ from predictions based on bulk oxide material properties. The interfacial electronic structure also influences the electrostatic potential distribution at the oxide–

TCO interface, which is often a critical operational aspect of working optoelectronic devices.

ZnO , as another wide band gap semiconductor, has also been widely investigated as a photoanode for PEC water splitting [17,18]. Different approaches, such as ion doping [19–21] and visible light sensitization with narrow band gap semiconductors [22–24], have been used to expand the light absorption region and hence improve the PEC performance for water splitting over ZnO anodes under solar light irradiation. Recently, a novel concept was demonstrated by our group, with ZnO nanostructures doped in core regions with shallow Al donor levels for enhanced electronic conduction and in the near-surface volume with intragap Ni impurity states for increased optical absorption [25]. In this study, we designed a novel isostructural ZnO:Al/ZnO:Ni core/shell nanorod structure for PEC water splitting, as shown in Fig. 5(a). The broad absorption features at long wavelengths in Fig. 5(b) overlapped with transitions associated with tetrahedrally coordinated Ni(II) in the ZnO lattice. Amperometric (current–time) measurements with application of color filters, as shown in Fig. 5(c), indicated that approximately 44% of total photocurrent originated from wavelengths beyond 410 nm, and 4.4% originated from beyond 510 nm. IPCE results in Fig. 5(d) showed that approximately a three-fold enhancement in conversion efficiencies for solar-abundant visible wavelengths was achieved over a ZnO:Al/ZnO:Ni core/shell structure by distributing the absorptive species normal to the substrate and along the direction of light propagation. The proposed band diagram and charge transfer processes within the core/shell structure were established in Fig. 5(e).

Hematite ($\alpha\text{-Fe}_2\text{O}_3$), known for its abundance, non-toxicity and exceptional chemical stability, is an increasingly promising material for solar-driven PEC water splitting, due to its narrow band gap of approximately 2.1 eV, enabling the absorption of a large portion of visible light in the incident solar spectrum. However, the poor charge transport property of $\alpha\text{-Fe}_2\text{O}_3$ greatly limits its efficiency as a photoanode for

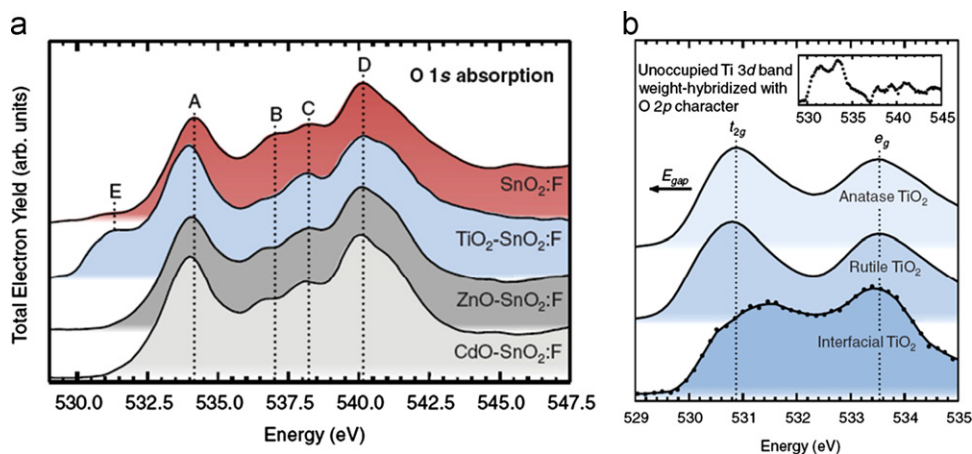


Fig. 3 (a) O K -edge x-ray absorption spectra for $\text{SnO}_2\text{:F}$ and the $\text{TiO}_2\text{-SnO}_2\text{:F}$, $\text{ZnO-SnO}_2\text{:F}$, and $\text{CdO-SnO}_2\text{:F}$ interfaces. Peak A corresponds to the O 2p orbitals hybridized with Sn 5s orbitals at the bottom of the conduction band. Peaks B, C, and D primarily correspond to the O 2p orbitals hybridized with Sn 5p orbitals deeper in the conduction band. Peak E results from the hybridization of unoccupied Ti $d(t_{2g})$ levels with O 2p levels, which exist in the conduction bands of titanium oxides. (b) Oxygen 1s absorption spectra for anatase TiO_2 , rutile TiO_2 , and TiO_2 thin film deposited on $\text{SnO}_2\text{:F}$. The interfacial TiO_2 spectrum was obtained by subtraction of the $\text{SnO}_2\text{:F}$ O 1s absorption spectrum such that the intensity remained positive. The dashed vertical lines indicate the energies of the Ti t_{2g} and e_g band maxima for anatase TiO_2 . The inset provides the interfacial TiO_2 spectrum at higher energies. Reprinted with permission from Ref. [16]. Copyright 2012 American Physical Society.

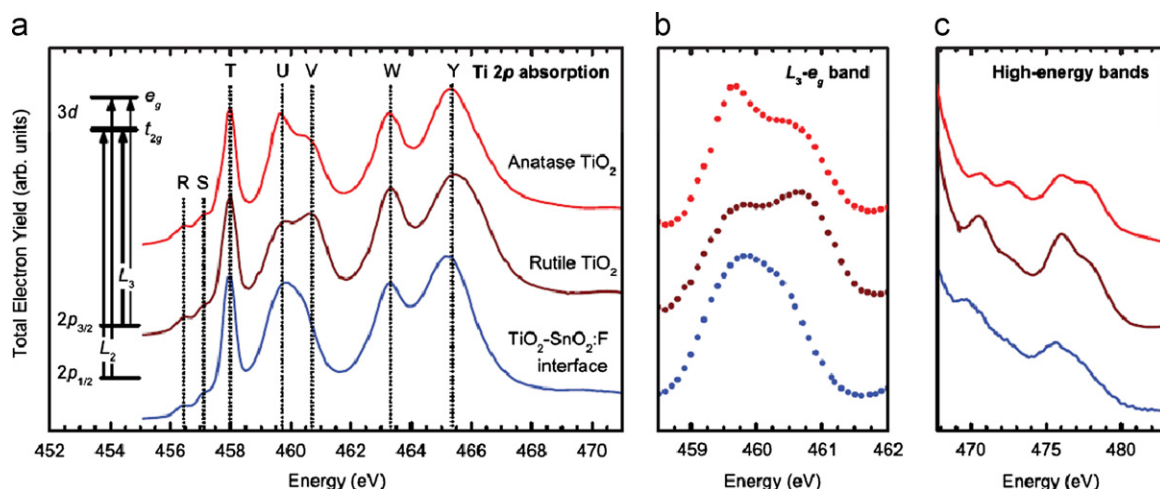


Fig. 4 Ti $L_{2,3}$ -edge x-ray absorption spectra for anatase TiO_2 (red), rutile TiO_2 (dark red), and $\text{TiO}_2\text{-SnO}_2\text{:F}$ (blue). (a) Complete spectra; (b) L_3 - e_g band; (c) high-energy bands, normalized to peak Y. (b) and (c) follow the same order and color convention as in (a). Peaks T and W reflect transitions to empty t_{2g} levels, and peaks U, V, and Y reflect transitions to empty e_g levels. The leading-edge multiplet structure of TiO_2 (peaks R and S) are assigned to $2p^6d^0 \rightarrow 2p^5d^1$ for Ti^{4+} in O_h symmetry. Reprinted with permission from Ref. [16]. Copyright 2012 American Physical Society.

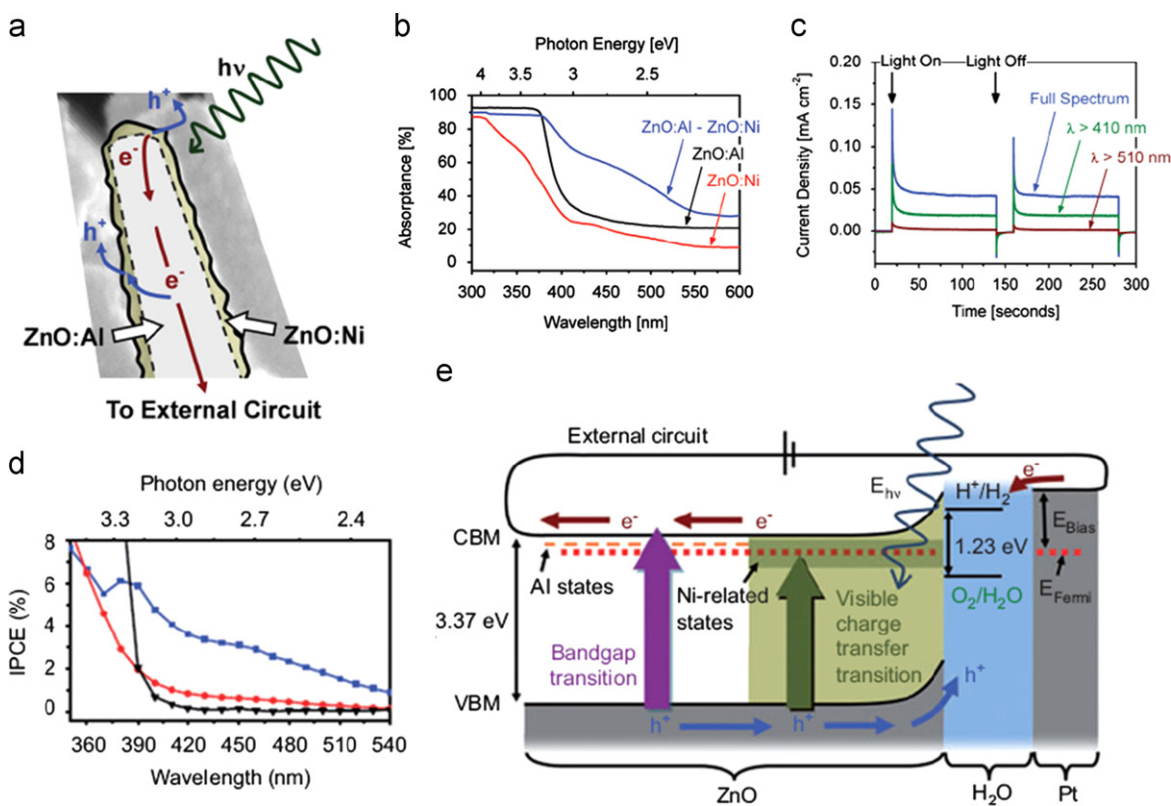


Fig. 5 (a) A schematic of idealized operating mechanisms overlaid onto the tip of an individual nanostructure. (b) Absorbance spectra of ZnO/FTO/glass structures. (c) Amperometric (current–time) measurement at 0.6 V versus Ag/AgCl with chopped AM 1.5 G-filtered 100 mW cm^{-2} irradiation, with application of wavelength filters. (d) Incident photon conversion efficiency at visible wavelengths for ZnO:Al–ZnO:Ni homojunction array (blue squares), ZnO:Ni thin film (red circles), and ZnO:Al nanorod array (black triangles), with +1 V applied versus a Pt counter electrode. (e) Idealized energetics of the functional homojunction nanostructure. Reprinted with permission from Ref. [25]. Copyright 2012 WILEY-VCH Verlag GmbH & Co. KGaA, Weinheim.

PEC water splitting. Thus, many different dopants have been employed to increase the electrical conductivity for improved PEC activity of $\alpha\text{-Fe}_2\text{O}_3$ [26]. In our group, the fabrication and

morphological, optical, and photoelectrochemical characterizations of doped $\alpha\text{-Fe}_2\text{O}_3$ films for solar water splitting have been carefully investigated. We deposited Ti-doped $\alpha\text{-Fe}_2\text{O}_3$

on FTO substrates by pulse laser deposition (PLD) in an oxygen environment at a moderate vacuum pressure of 4 mTorr, from a $\text{Fe}_2\text{O}_3\text{:TiO}_2$ target [27]. We determined that despite the apparent increased surface area, porous electrodes deposited at 23 °C were significantly less efficient than denser electrodes deposited at 300 °C. It is hoped that such a finding is applicable to future studies of the fabrication of efficient iron oxide-based photoanodes, which is known to require careful film growth engineering. We also successfully tuned the surface composition of $\alpha\text{-Fe}_2\text{O}_3$ nanorod arrays modified by doping of Cr^{3+} or W^{6+} using a general process involving a combination of aqueous chemical growth and spin coating [28,29]. The photoluminescence spectra indicated that photocurrent enhancement was mainly due to the enhanced charge transfer in the surface tuned $\alpha\text{-Fe}_2\text{O}_3$ nanorods, as shown in Fig. 6 (taking Cr^{3+} doping as an example). We also paid particular attention to one-dimensional core/shell nanorod structures, as structures of this type are most likely to utilize the benefits afforded by designed surface overlayer coating and are likely to show functional behavior relating to the core/shell interfacial region. Novel core/shell nanoarrays, based on $\alpha\text{-Fe}_2\text{O}_3$ nanorods with the surface modified by a thin WO_3 or TiO_2 overlayer, were fabricated by a combination of aqueous chemical synthesis and vapor phase deposition [30,31]. The enhanced photoelectrochemical activity of the $\alpha\text{-Fe}_2\text{O}_3/\text{WO}_3$ core/shell structure indicated that the modification of $\alpha\text{-Fe}_2\text{O}_3$ nanorods with WO_3 overlayer promoted the extraction of surface-trapped holes from the $\alpha\text{-Fe}_2\text{O}_3$ core [30]. This should be directly related to the unique features of the core/shell nanoscale architecture, such as interface electronic orbital reconstruction via $p\text{-}d$ orbital hybridization as well as quantum-mechanical tunneling. Further formation revealed that core/shell heterostructures, comprised of an $\alpha\text{-Fe}_2\text{O}_3$ core coated with a TiO_2 overlayer, resulting in an emergent degree of $p\text{-}d$ orbital hybridization and spontaneous electron enrichment in the interfacial region and thus possessed a unique electronic structure [31].

WO_3 is also a visible-light-sensitive anode material attractive for PEC water splitting [32]. Studies have mainly focused on nanostructure and heterojunction design for the outstanding PEC performances of WO_3 films [32,33]. The authors' colleagues in Xi'an Jiaotong University (XJTU), China, successfully synthesized WO_3 nanowire arrays using a solvothermal technique on FTO substrates [34]. WO_3 morphologies of hexagonal and monoclinic structure, ranging from nanowire to nanoflake

arrays, could be tailored by adjusting solution composition with growth along the (001) direction. Photoelectrochemical measurements showed incident photon-to-current conversion efficiencies higher than 60% at 400 nm with a photocurrent of 1.43 mA/cm^2 under AM 1.5 G illumination. They further coupled WO_3 with BiVO_4 , which has a smaller band gap, by spin coating [35]. The heterojunction structure offered enhanced photoconversion efficiency and increased photocorrosion stability. Compared to planar $\text{WO}_3/\text{BiVO}_4$ heterojunction films, the nanorod-array films showed significantly improved photoelectrochemical properties due to the high surface area and improved separation of the photogenerated charge at the $\text{WO}_3/\text{BiVO}_4$ interface.

3. Nano-photocatalysts for hydrogen production

In 1979, the concept of photoelectrochemical water splitting was applied by Bard to design a photocatalytic water splitting system using semiconductor particles or powders as photocatalysts [36]. In the photocatalytic system as depicted in Fig. 7, electrons and holes photogenerated in the conduction band and valence band transfer to the surface of particulate photocatalysts, and then partake in a redox reaction, producing hydrogen and oxygen, respectively [5]. By looking into the basic mechanism and process of photocatalytic water splitting, one could find that efficient photocatalysts should have (1) suitable band gaps and band structures to absorb abundant solar light to drive hydrogen- and oxygen-evolution half-reactions; (2) good charge transfer ability for electrons and holes moving to the semiconductor/electrolyte interface with retarded charge recombination; and (3) high surface catalytic reactivity for half-reactions. In the past decades, numerous efforts have been dedicated to meet these critical requirements of photocatalysts designed for high efficiency hydrogen production from water [5,37–41]. In this section, research progress in our group on the design of nano-photocatalysts for hydrogen production was introduced, showing our great efforts and professional ideas to advance this technology, applicable for high-efficiency and low-cost solar fuel production in the near future.

As discussed in the previous section, TiO_2 , as the most studied wide band gap photocatalyst, has been extensively doped with ions to narrow its band gap for efficient visible light photocatalytic hydrogen production [6]. However, the

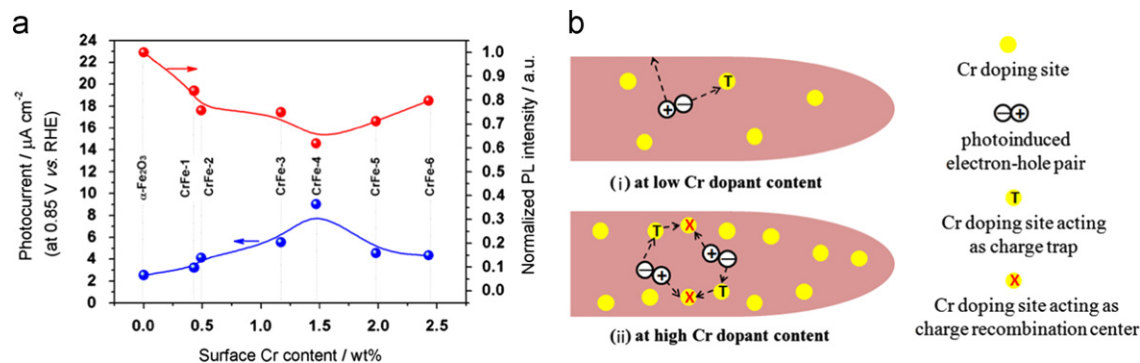


Fig. 6 (a) Photocurrent and photoluminescence intensity as a function of Cr dopant content for Cr-doped $\alpha\text{-Fe}_2\text{O}_3$ nanorod films. (b) Proposed schemes for photoinduced charge transfer in the Cr-doped $\alpha\text{-Fe}_2\text{O}_3$ nanorod films with different Cr dopant contents, (i) at low Cr dopant content and (ii) at high Cr dopant content. Reprinted with permission from Ref. [29]. Copyright 2012 Elsevier.

doping-created energy levels could act as recombination centers for photoinduced charges, which would seriously limit the photocatalytic activity of doped TiO₂. Recently, our group put forward a conceptually novel approach to enhance solar absorption of TiO₂ nanocrystals by introducing disorder in the

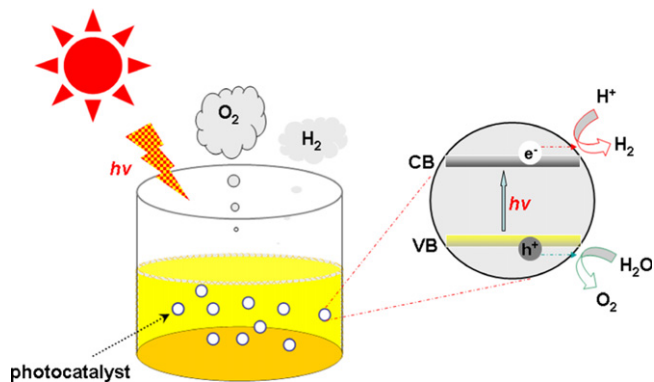


Fig. 7 Illustrated scheme of photocatalytic water splitting.

surface layers [42]. With anatase TiO₂ crystals of *ca.* 8 nm in diameter hydrogenated in a 20.0-bar H₂ atmosphere at 200 °C for 5 days, the obtained black TiO₂ nanocrystals had the surfaces disordered, where the disordered outer layer surrounding a crystalline core was about 1 nm in thickness as depicted in Fig. 8(a). From Fig. 8(b) it is clear that the band gap of the unmodified white TiO₂ nanocrystals was *ca.* 3.30 eV, while the onset of optical absorption of the black disorder-engineered TiO₂ nanocrystals was shifted to \sim 1200 nm, suggesting that the optical gap was substantially narrowed to be *ca.* 1.0 eV by intraband transitions, as illustrated in Fig. 8(c). A 22 day test demonstrated that black TiO₂ nanocrystals produced hydrogen continuously at a steady rate, as shown in Fig. 8(d). This hydrogen production rate (10 m mol h⁻¹ g⁻¹ of photocatalysts), with a solar energy conversion efficiency as high as 24%, is about 2 orders of magnitude greater than the yields of most semiconductor photocatalysts [5,40]. This could be attributed to the efficient harvest of photons from UV to near-infrared by the disorder-engineered black TiO₂ for photocatalysis, and the retarded charge recombination due to the localization of both photoexcited electrons and holes.

Photocatalytic activity is strongly dependent on the photoinduced charge transport and separation efficiencies in the

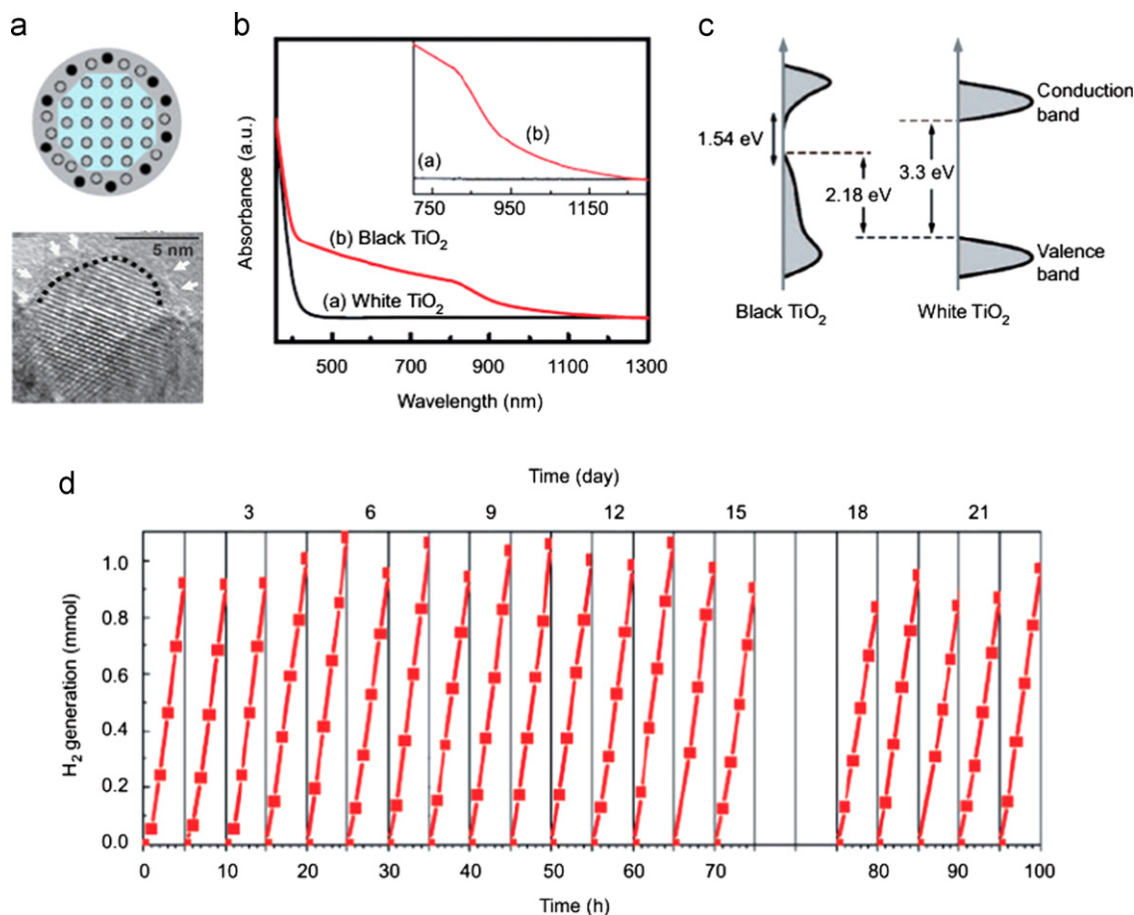


Fig. 8 (a) Schematic illustration and TEM image of the structure of disorder-engineered black TiO₂. (b) Spectral absorbance of the white and black TiO₂ nanocrystals. The inset enlarges the absorption spectrum in the range from approximately 750–1200 nm. (c) Schematic illustration of the DOS of disorder-engineered black TiO₂ nanocrystals, as compared to that of unmodified TiO₂ nanocrystals. (d) Cycling measurements of hydrogen gas generation through direct photocatalytic water splitting with disorder-engineered black TiO₂ nanocrystals under simulated solar light. Experiments were conducted over a 22 day period, with 100 h of overall solar irradiation time. Reprinted with permission from Ref. [42]. Copyright 2011 American Association for the Advancement of Science.

photocatalysts. To promote charge separation, semiconductor heterojunctions have been frequently designed to create an electrostatic field for directional migration of electrons and holes [5,43]. However, these heterojunctions will hinder the transport capability of free charges [44]. Therefore, in recent years, our group has focused on the microstructured refinement of semiconductor photocatalysts, aiming at promoting charge separation as well as facilitating charge transport. We systematically investigated the effects of synthetic conditions on the microstructure and hence photocatalytic activity of ZnIn_2S_4 for hydrogen evolution under visible-light irradiation [45–47], and found the $d(001)$ space and internal electrostatic field of ZnIn_2S_4 were controllably tuned. The $d(001)$ space increased, leading to the increasing distortion extent of $[\text{ZnS}_4]$ and $[\text{InS}_4]$ tetrahedron in ZnIn_2S_4 structure, the internal electrostatic fields induced by dipole moment increased, which was considered useful for electron–hole separation and hence beneficial to photocatalytic hydrogen production. $\text{Cd}_{1-x}\text{Zn}_x\text{S}$ solid solutions with nano-twin structures (Fig. 9(a)) were synthesized by our colleagues in XJTU and exhibited superior photocatalytic activities for hydrogen evolution from water under visible light irradiation without noble metals, with an extremely high apparent quantum yield of 43% at 425 nm [48]. As shown in Fig. 9(b), the “back to

back” potential formed by parallel nano-twins in the $\text{Cd}_{1-x}\text{Zn}_x\text{S}$ crystals could significantly improve the separation of the photo-generated electrons and holes and thus enhance photocatalytic activity. The concentration of free electrons at the central region of the twins was markedly higher; the twins can effectively separate the H_2 evolution sites (electrons) from oxidation reaction sites (holes).

Loading cocatalysts onto photocatalysts to form hydrogen or oxygen evolution sites have been considered as an effective method to enhance photocatalytic activity for water splitting. In the past decades, different kinds of materials such as transition metals (especially the noble metals), metal oxides, and metal sulfides have been developed as effective cocatalysts for photocatalytic water splitting [5,38]. It is well known that some noble metals, such as Pt, Ru, Au, etc., and metal oxides, such as NiO_x , $\text{Rh}/\text{Cr}_2\text{O}_3$, etc., perform well as water reduction cocatalysts by entrapping electrons from semiconductors; while many other metal oxides, such as IrO_2 , RuO_2 , Rh_2O_3 , Co_3O_4 , and Mn_3O_4 , have performed as effective oxidation cocatalysts by entrapping holes [37]. In our studies on the screening of cocatalysts for photocatalytic hydrogen production, we found that loading noble metals and metal sulfides

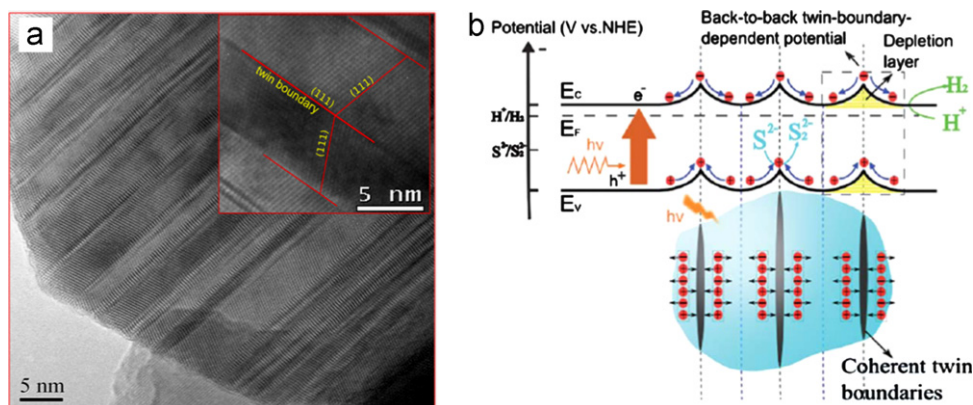


Fig. 9 (a) TEM image of $\text{Cd}_{1-x}\text{Zn}_x\text{S}$ solid solutions with nano-twin structures. (b) Parallel boundaries provided twin boundary-dependent potential, which derived the “back to back” Schottky barrier and would control the migration of free charges. Reprinted with permission from Ref. [48]. Copyright 2011 Royal Society of Chemistry.

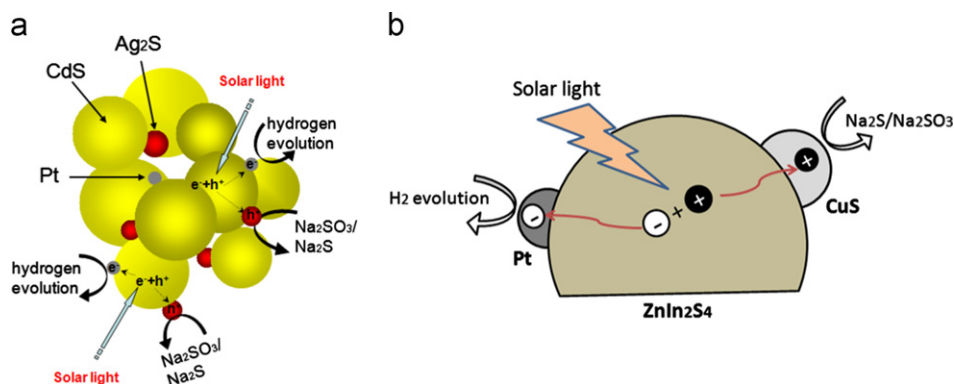


Fig. 10 Schematic illustration of the photo-generated charge transfer process for photocatalytic hydrogen evolution over (a) Pt– Ag_2S co-loaded CdS, and (b) Pt–CuS co-loaded ZnIn_2S_4 , from an aqueous solution containing $\text{Na}_2\text{SO}_3/\text{Na}_2\text{S}$ under simulated solar light. Reprinted with permission from Ref. [49]. Copyright 2010 Elsevier. Reprinted with permission from Ref. [50]. Copyright 2011 Springer.

as dual cocatalysts (Pt–Ag₂S and Pt–CuS), which acted as reduction and oxidation cocatalysts by entrapping electrons and holes from semiconductors (Fig. 10), respectively, could cause more efficient separation of photogenerated electrons and holes, and hence resulting in enhanced photocatalytic activity for hydrogen evolution [49,50].

4. Solid-state nanomaterials for hydrogen storage

As discussed in the previous two sections, hydrogen can be sustainably converted from solar energy via a photochemistry process. However, hydrogen storage also remains as one of the key challenges to realize hydrogen economy. In general, hydrogen can be stored as pressurized gas, cryogenic liquid, or in a suitable solid-state material such as metal hydrides, metal–organic frameworks and carbon materials [51–53]. Compared to the two former approaches of gaseous and liquid-state hydrogen storage, solid-state hydrogen storage could be done at near-ambient temperatures and pressures with hydrogen chemically or physically absorbed to the solid-state materials. Moreover, storage of hydrogen in liquid or gaseous form requires a large container and poses important safety problems for on-board transport applications. Therefore, solid-state storage is potentially the most convenient and the safest method from a technological point of view. For solid-state hydrogen storage, the storage capacity and kinetics strongly depend on material-specific surface interactions, no matter how hydrogen binds to surfaces of solid-state materials, either strong chemical associations (chemisorption) or weak dispersive interactions (physisorption) [54,55].

Although limited by high thermodynamic stability or poor reaction kinetics, metal hydrides, as the reversible chemisorption materials, represent an important class of candidate materials for solid-state hydrogen storage due to high formula hydrogen storage capacities [56]. MgH₂ is of particular interest due to the abundance of Mg and the relatively high hydrogen weight percentage (7.6%). However, due to its high enthalpy of formation, bulk MgH₂ generally does not release hydrogen below 300 °C. Therefore, a reduction in the enthalpy of formation is required to improve the thermodynamics of an MgH₂ based system to make it a viable candidate for hydrogen storage application. A common method to address this high enthalpy problem is to alloy Mg with metals such as Ni or Al [57,58], however, this negatively leads to a significant

reduction in the hydrogen weight percentage. In our group, an Mg nanoparticle layer in the form of sandwiched Pd/Mg/Pd thin films was deposited using the PLD method, as shown in Fig. 11(a) [59]. This nanoparticle film could reduce the enthalpy of formation and the thermodynamic barrier to hydride formation, complementing the enhanced kinetics from the Pd layers. The reduction of the formation enthalpy could be explained by the concept of excess volume associated with a film of nanoparticles. Both the metal and the metal hydride phase can be destabilized by excess volume. The enthalpy of formation of the hydride phase will only decrease if the metal hydride phase is more destabilized than the metal phase (Fig. 11(b)). While further reduction is necessary for practical applications, substrate-free thin films appear to be a useful approach for exploring new metal hydride materials for hydrogen storage. Thus, we fabricated free-standing Mg–Ni films with extensive nanoscale grain structures using a combination of pulsed laser deposition and film delaminating processes [60]. Oxidation of the material was reduced through the use of a sandwiched free-standing film structure in which the top and bottom layers consist of nanometer-thick Pd layers, which also act as a catalyst to promote hydrogen uptake and release. An improvement in hydrogen storage capacity over the bulk Mg–Ni target material was found for the free-standing films, while the thermodynamic stability of the nanograined films was similar to that of Mg₂Ni. These results suggest that free-standing films, of which better control of material compositions and microstructures can be realized is possible for conventional ball-milled powders, represent a useful materials platform for solid-state hydrogen storage research.

To offer an advantage in studying multi-component alloys and their phase transition to metal hydrides, high throughput materials fabrication and characterization techniques were developed in our group [61]. We fabricated an Mg–Ni–Al and Ca–B–Ti ternary alloy libraries using a continuous combinatorial material synthesis technique, and measured the optical reflectance to examine the formation of the metal hydride phase when the alloy library was exposed to hydrogen. The results indicate that mapping the change in reflectance is a viable method to study the kinetics of hydride formation. Monitoring the optical properties provides evidence for the “black state” formed during the transition from the α -phase to β -phase. In addition, we found that the fastest reflectance change occurred when the alloy has an Mg to Ni

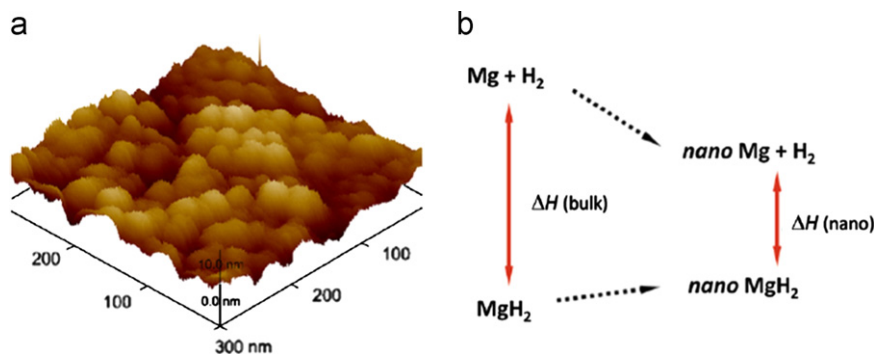


Fig. 11 (a) A typical AFM image of Mg nanoparticle film without a Pd capping layer. (b) Schematic illustration of the reduction of the enthalpy of formation with both Mg and MgH₂ destabilized. Reprinted with permission from Ref. [59]. Copyright 2010 Elsevier.

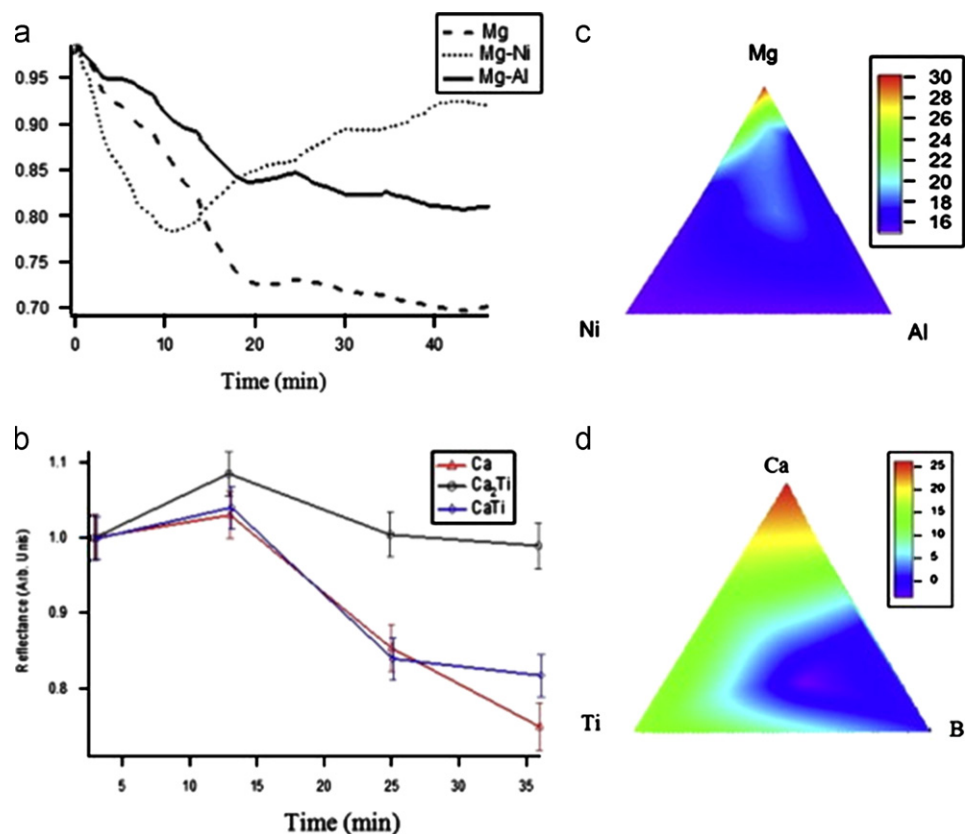


Fig. 12 (a) Time-resolved reflectance measurements at 323 K in 300 psi H₂. The Mg–Ni and Mg–Al curves are taken from a region at roughly 2Mg for each Ni or Al atom, respectively. (b) Percent decrease in reflectance after 1 h in 300 psi H₂ at 323 K. (c) Time-resolved reflectance from the Ca–Ti region of a Ca–B–Ti sample in 300 psi H₂ at 473 K. (d) Percent change in reflectance after 1 h at 473 K in 300 psi H₂. Reprinted with permission from Ref. [61]. Copyright 2010 Elsevier.

ratio of approximately 2:1, and with low concentration of Al (Fig. 12(a,b)). Initial testing of a Ca–B–Ti sample indicates that some reaction has occurred in the Ca and Ti regions under slightly higher temperature conditions than were required for Mg–Ni–Al (Fig. 12(c,d)). The high throughput optical reflectance method developed here would be a valuable tool for screening metal hydride materials with the goal of practical hydrogen storage applications.

Mesoporous materials offer several advantages over other materials due to their large surface area, open porosity, small pore sizes, and the ability to coat the surface of the mesoporous structure with one or more compounds. For example, with exceptionally high surface areas and chemically-tunable structures, metal–organic frameworks have recently emerged as some of the most promising candidate materials for physisorption hydrogen storage [62]. We have been investigating the preparation and properties of ultra-low density nanomaterials based on the aerogel technology for many years. Using this technology, we have prepared a wide variety of aerogel compositions including metal oxides (SiO₂, TiO₂, Fe₃O₄, Al₂O₃, MgO, Cr₂O₃, and Zr₂O₃), mixed oxides, and other compounds [63]. Moreover, aerogels can be readily modified by incorporating transition metals into the oxide network. We found that the SiO₂ nanoparticle networks could store hydrogen up to 2.5 wt% through physisorption at liquid nitrogen temperature, due to their very large surface area [64,65]. To

increase the density of stored hydrogen we introduced chemisorption into SiO₂ nanoparticle networks, while maintaining the benefit of the high-surface area for additional storage through functionalized physisorption. At the same time, the high-surface area nanoparticle network provided the additional benefit of markedly improved chemisorption kinetics by increasing reaction surface area as well as reducing diffusion distance. We fabricated a composite material using MgNi (<5 wt%) implemented in an ultralow-density SiO₂ aerogel nanoparticle network. Preliminary measurements indicated chemisorption of hydrogen in the modified silica network, in addition to physisorption due to very large surface area offered by the oxide network. With the scale-up manufacturing feasibility of nanostructured oxide networks based on the aerogel technology, ultralow density active ceramic networks represent a clear alternative to existing porous media for solid-state hydrogen storage [65].

5. Nano-electrocatalyst for PEMFCs

As clean energy conversion devices, proton exchange membrane (or polymer electrolyte membrane) fuel cells (PEMFCs) can harness the chemical energy of hydrogen to generate electricity at a high-energy conversion efficiency of greater than 70% without combustion and pollution. These advantages render PEMFCs an attractive replacement for

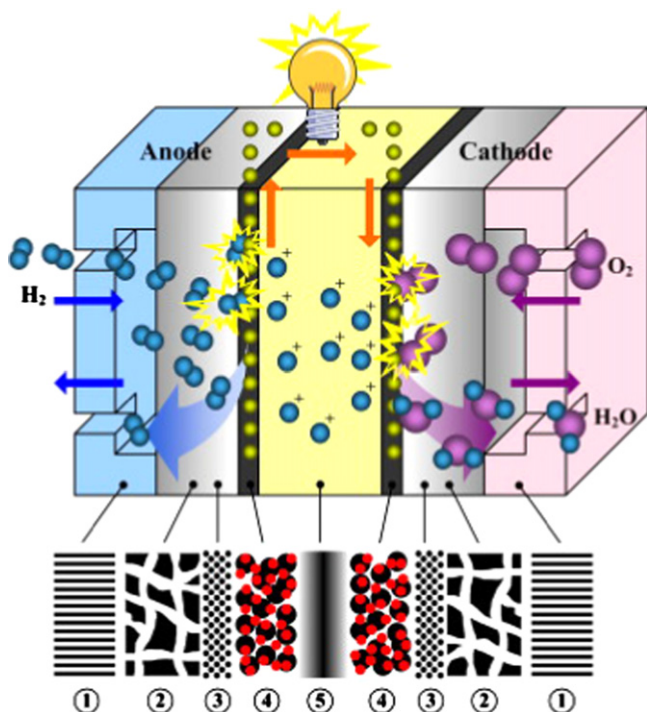


Fig. 13 Schematic of the working principle of a typical PEMFC (direct hydrogen) and the involved porous components. (1)—Bipolar plate; (2)—backing layer; (3)—microporous layer; (4)—electrocatalyst layer; and (5)—membrane. Reprinted with permission from Ref. [66]. Copyright 2012 Elsevier.

combustion engines for both mobile and stationary applications. Fig. 8 is a schematic illustration of the basic structure and the operation principle of a typical PEMFC [66]. In operation, hydrogen is ionized on the anode to produce electrons and protons. The protons move through the membrane, while the electrons move through an external circuit. The protons and electrons recombine on the cathode, reducing oxygen

to water in the process [67]. As shown in Fig. 13, attached to either side of the electrolyte membrane are porous gas diffusion electrodes consisting of the catalytic active layer with electrocatalysts.

Due to the slow kinetics of the oxygen reduction reaction on the cathode, which is primarily responsible for high voltage losses in a PEMFC and therefore low conversion efficiency, effective electrocatalysts are required to enhance the rate of the reaction. Moreover, electrocatalysts must be durable in an acidic environment for the continuous operation of PEMFCs. Platinum (Pt) has been regarded as the most active catalyst for the oxygen reduction reaction. However, the high cost and scarcity of Pt greatly limits the development and widespread commercialization of PEMFCs [68]. Thus, in the past decades, low-Pt containing alloys have been made to reduce Pt usage in the fuel cell cathode [69,70], and different kinds of non-Pt electrocatalysts such as metal chalcogenides, metal oxides, metal carbides and nitrides, and macrocycles, have been proposed as alternatives to replace noble metals in PEMFCs [71]. Of these non-Pt electrocatalysts, chromium nitrides such as CrN and Cr₂N have been considered as potential electrocatalysts, due to their high resistance to wear and corrosion [72,73]. We demonstrated that highly crystalline

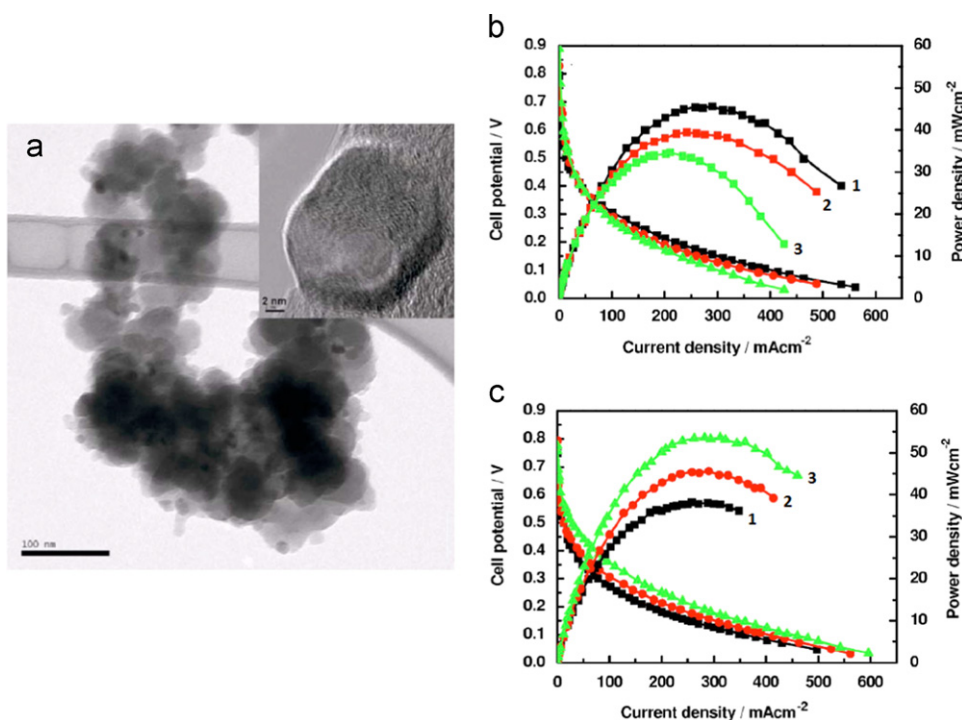


Fig. 14 (a) TEM images of CrN/C prepared at 800 °C. The inset shows a high resolution TEM image of a single CrN nanocrystal. (b) Polarization curves of fuel cell devices with CrN loading of 0.5 mg cm⁻² prepared at different temperatures: (1) 800 °C, (2) 900 °C, and (3) 950 °C. (c) Polarization curves with different CrN loadings: (1) 0.42 mg cm⁻², (2) 0.5 mg cm⁻², and (3) 1.08 mg cm⁻² at 800 °C. Reprinted with permission from Ref. [74]. Copyright 2007 American Institute of Physics.

CrN nanoparticles of fcc structure exhibited attractive catalytic activity and stability for the oxygen reduction reaction in PEMFCs, as shown in Fig. 14 [74]. Experiments on the reaction kinetics of CrN-based electrodes indicated a combined kinetic diffusion mechanism of charge and mass transport. The oxygen was partially reduced to H₂O via the four-electron route at the CrN electrode, and partially reduced to H₂O₂ and then H₂O via the two-electron route. Although the catalytic activity of CrN nanocrystals is somewhat lower than that of Pt, their resource is abundant in addition to their much lower cost. Optimization in nitride preparation processes, including composition variations could potentially enhance their catalytic activity, which makes nitride nanocrystals promising for PEMFCs [74].

6. Concluding remarks

Along with the continuous research on developing novel concepts and technologies with renewable energy application, in the past decades there have been numerous attempts to develop nanomaterials to achieve applicable renewable energy conversion and utilization. The examples discussed in this article provide the state-of-the-art concepts of nanomaterial design for high efficiency photocatalytic/photoelectrochemical solar hydrogen conversion, high capacity hydrogen storage, and effective electricity generation from fuel cells. Although there are still many challenges ahead in these areas, the review article presented here demonstrates that nanomaterial design is important for future research into these selected technologies for renewable energy. In the long-term nanomaterial research can contribute to an eventual transition into a renewable energy (*e.g.* solar and hydrogen) based economy.

Acknowledgment

This work has been supported by the US Department of Energy, Office of Energy Efficiency and Renewable Energy.

References

- [1] L. Vayssieres, *On Solar Hydrogen and Technology*, John Wiley and Sons, Singapore, 2009.
- [2] S.S. Mao, X. Chen, Selected nanotechnologies for renewable energy applications, *International Journal of Energy Research* 31 (2007) 619–636.
- [3] F.D.S. Marquis, The role of nanomaterials systems in energy and environment: renewable energy, *Journal of the Minerals Metals and Materials Society* 63 (2011) 43.
- [4] A. Fujishima, K. Honda, Electrochemical photolysis of water at a semiconductor electrode, *Nature* 238 (1972) 37–38.
- [5] X. Chen, S. Shen, L. Guo, S.S. Mao, Semiconductor-based photocatalytic hydrogen generation, *Chemical Reviews* 110 (2010) 6503–6570.
- [6] X. Chen, S.S. Mao, Titanium dioxide nanomaterials: synthesis, properties, modifications, and applications, *Chemical Reviews* 107 (2007) 2891–2959.
- [7] M. Ni, M.K.H. Leung, D.Y.C. Leung, K. Sumathy, A review and recent developments in photocatalytic water-splitting using TiO₂ for hydrogen production, *Renewable and Sustainable Energy Reviews* 11 (2007) 401–425.
- [8] S.U.M. Khan, M. Al-Shahry, W.B. Ingler Jr., Efficient photochemical water splitting by a chemically modified *n*-TiO₂, *Science* 297 (2002) 2243–2245.
- [9] S. Rani, S.C. Roy, M. Paulose, O.K. Varghese, G.K. Mor, S. Kim, S. Yoriya, T.J. LaTempa, C.A. Grimes, Synthesis and applications of electrochemically self-assembled titania nanotube arrays, *Physical Chemistry Chemical Physics* 12 (2010) 2780–2800.
- [10] G.K. Mor, H.E. Prakasham, O.K. Varghese, K. Shankar, C.A. Grimes, Vertically oriented Ti–Fe–O nanotube array films: toward a useful material architecture for solar spectrum water photoelectrolysis, *Nano Letters* 7 (2007) 2356–2364.
- [11] G.K. Mor, K. Shankar, M. Paulose, O.K. Varghese, C.A. Grimes, Enhanced photocleavage of water using titania nanotube arrays, *Nano Letters* 5 (2005) 191–195.
- [12] O.K. Varghese, M. Paulose, K. Shankar, G.K. Mor, C.A. Grimes, Water-photolysis properties of micron-length highly-ordered titania nanotube-arrays, *Journal of Nanoscience and Nanotechnology* 5 (2005) 1158–1165.
- [13] K. Shankar, G.K. Mor, H.E. Prakasham, S. Yoriya, M. Paulose, O.K. Varghese, C.A. Grimes, Highly-ordered TiO₂ nanotube arrays up to 220 μm in length: use in water photoelectrolysis and dye-sensitized solar cells, *Nanotechnology* 18 (2007) 065707.
- [14] M. Paulose, K. Shankar, S. Yoriya, H.E. Prakasham, O.K. Varghese, G.K. Mor, T.A. Latempa, A. Fitzgerald, C.A. Grimes, Enhanced photocleavage of water using titania nanotube arrays, *Journal of Physical Chemistry B* 110 (2006) 16179–16184.
- [15] G.K. Mor, O.K. Varghese, R.H.T. Wilke, S. Sharma, K. Shankar, T.J. Latempa, K.S. Choi, C.A. Grimes, *p*-Type Cu–Ti–O nanotube arrays and their use in self-biased heterojunction photoelectrochemical diodes for hydrogen generation, *Nano Letters* 8 (2008) 1906–1911.
- [16] C.X. Kronawitter, M. Kapilashrami, J.R. Bakke, S.F. Bent, C.-H. Chuang, W.-F. Pong, J. Guo, L. Vayssieres, S.S. Mao, TiO₂–SnO₂:F interfacial electronic structure investigated by soft x-ray absorption spectroscopy, *Physical Review B* 85 (2012) 125109.
- [17] A.I. Hochbaum, P. Yang, Semiconductor nanowires for energy conversion, *Chemical Reviews* 110 (2010) 527–546.
- [18] Y.J. Lin, G.B. Yuan, R. Liu, S. Zhou, S.W. Sheehan, D.W. Wang, Semiconductor nanostructure-based photoelectrochemical water splitting: a brief review, *Chemical Physics Letters* 507 (2011) 209–215.
- [19] X. Yang, A. Wolcott, G. Wang, A. Sobo, R.C. Fitzmorris, F. Qian, J.Z. Zhang, Y. Li, Nitrogen-doped ZnO nanowire arrays for photoelectrochemical water splitting, *Nano Letters* 9 (2009) 2331–2336.
- [20] S. Shet, K.S. Ahn, R. Nugehalli, Y.F. Yan, J. Turner, M. Al-Jassim, Phase separation in Ga and N co-incorporated ZnO films and its effects on photo-response in photoelectrochemical water splitting, *Thin Solid Films* 519 (2011) 5983–5987.
- [21] M. Yousefi, M. Amiri, R. Azimirad, A.Z. Moshfegh, Enhanced photoelectrochemical activity of Ce doped ZnO nanocomposite thin films under visible light, *Journal of Electroanalytical Chemistry* 661 (2011) 106–112.
- [22] H. Kim, M. Seol, J. Lee, K. Yong, Highly efficient photoelectrochemical hydrogen generation using hierarchical ZnO/WO_x nanowires cosensitized with CdSe/CdS, *Journal of Physical Chemistry C* 115 (2011) 25429–25436.
- [23] G. Wang, X. Yang, F. Qian, J.Z. Zhang, Y. Li, Double-sided CdS and CdSe quantum dot co-sensitized ZnO nanowire arrays for photoelectrochemical hydrogen generation, *Nano Letters* 10 (2010) 1088–1092.
- [24] N. Chouhan, C.L. Yeh, S.-F. Hu, R.-S. Liu, W.-S. Chang, K.-H. Chen, Photocatalytic CdSe QDs-decorated ZnO nanotubes: an effective photoelectrode for splitting water, *Chemical Communications* 47 (2011) 3493–3495.
- [25] C.X. Kronawitter, Z. Ma, D. Liu, S.S. Mao, B.R. Antoun, Engineering impurity distributions in photoelectrodes for solar water oxidation, *Advanced Energy Materials* 2 (2012) 52–57.
- [26] K. Sivula, F. Le Formal, M. Grätzel, Solar water splitting: PROgress using hematite (α -Fe₂O₃) photoelectrodes, *ChemSusChem* 4 (2011) 432–449.

- [27] C.X. Kronawitter, S.S. Mao, B.R. Antoun, Doped, porous iron oxide films and their optical functions and anodic photocurrents for solar water splitting, *Applied Physics Letters* 98 (2011) 092108.
- [28] S. Shen, C.X. Kronawitter, J. Jiang, S.S. Mao, L. Guo, Surface tuning for promoted charge transfer in hematite nanorod arrays as water-splitting photoanodes, *Nano Research* 5 (2012) 327–336.
- [29] S. Shen, J. Jiang, P. Guo, C.X. Kronawitter, S.S. Mao, L. Guo, Effect of Cr doping on the photoelectrochemical performance of hematite nanorod photoanodes, *Nano Energy* (2012).
- [30] C.X. Kronawitter, L. Vayssieres, S. Shen, L. Guo, D.A. Wheeler, J.Z. Zhang, B.R. Antoun, S.S. Mao, A perspective on solar-driven water splitting with all-oxide hetero-nanostructures, *Energy and Environmental Science* 4 (2011) 3889–3899.
- [31] C.X. Kronawitter, J.R. Bakke, D.A. Wheeler, W.C. Wang, C. Chang, B.R. Antoun, J.Z. Zhang, J. Guo, S.F. Bent, S.S. Mao, L. Vayssieres, Electron enrichment in 3d transition metal oxide hetero-nanostructures, *Nano Letters* 11 (2011) 3855–3861.
- [32] X. Liu, F. Wang, Q. Wang, Nanostructure-based WO₃ photoanodes for photoelectrochemical water splitting, *Physical Chemistry Chemical Physics* 14 (2012) 7894–7911.
- [33] B.D. Alexander, P.J. Kulesza, I. Rutkowska, R. Solarzka, J. Augustynski, Metal oxide photoanodes for solar hydrogen production, *Journal of Materials Chemistry* 18 (2008) 2298–2303.
- [34] J. Su, X. Feng, J.D. Sloppy, L. Guo, C.A. Grimes, Vertically aligned WO₃ nanowire arrays grown directly on transparent conducting oxide coated glass: Synthesis and photoelectrochemical properties, *Nano Letters* 11 (2011) 203–208.
- [35] J. Su, L. Guo, N. Bao, C.A. Grimes, Nanostructured WO₃/BiVO₄ heterojunction films for efficient photoelectrochemical water splitting, *Nano Letters* 11 (2011) 1928–1933.
- [36] A.J. Bard, Photoelectrochemistry and heterogeneous photocatalysis at semiconductors, *Journal of Photochemistry* 10 (1979) 59–75.
- [37] S. Shen, S.S. Mao, Nanostructure designs for effective solar-to-hydrogen conversion, *Nanophotonics* 1 (2012) 31–50.
- [38] S. Shen, J. Shi, P. Guo, L. Guo, Visible-light-driven photocatalytic water splitting on nanostructured semiconducting materials, *International Journal of Nanotechnology* 8 (2011) 523–591.
- [39] F.E. Osterloh, Inorganic materials as catalysts for photochemical splitting of water, *Chemistry of Materials* 20 (2008) 35–54.
- [40] A. Kudo, Y. Miseki, Heterogeneous photocatalyst materials for water splitting, *Chemical Society Reviews* 38 (2009) 253–278.
- [41] K. Maeda, K. Domen, Photocatalytic water splitting: recent progress and future challenges, *Journal of Physical Chemistry Letters* 1 (2010) 2655–2661.
- [42] X. Chen, L. Liu, P.Y. Yu, S.S. Mao, Increasing solar absorption for photocatalysis with black hydrogenated titanium dioxide nanocrystals, *Science* 331 (2011) 746–750.
- [43] J.S. Jang, H.G. Kim, J.S. Lee, Heterojunction semiconductors: a strategy to develop efficient photocatalytic materials for visible light water splitting, *Catalysis Today* 185 (2012) 270–277.
- [44] J.P. Schaffer, A. Saxena, S.D. Antolovich, T.H. Sanders, S. Warner, *The Science and Design of Engineering Materials*, McGraw-Hill, New York, 1999.
- [45] S. Shen, L. Zhao, L. Guo, Morphology, structure and photocatalytic performance of ZnIn₂S₄ synthesized via a solvothermal/hydrothermal route in different solvents, *Journal of Physics and Chemistry of Solids* 69 (2008) 2426–2432.
- [46] S. Shen, L. Zhao, L. Guo, Cetyltrimethylammoniumbromide (CTAB)-assisted hydrothermal synthesis of ZnIn₂S₄ as an efficient visible-light-driven photocatalyst for hydrogen production, *International Journal of Hydrogen Energy* 33 (2008) 4501–4510.
- [47] S. Shen, L. Zhao, L. Guo, Crystallite, optical and photocatalytic properties of visible-light-driven ZnIn₂S₄ photocatalysts synthesized via a surfactant-assisted hydrothermal method, *Materials Research Bulletin* 44 (2009) 100–105.
- [48] M. Liu, L. Wang, G. Lu, X. Yao, L. Guo, Twins in Cd_{1-x}Zn_xS solid solution: Highly efficient photocatalyst for hydrogen generation from water, *Energy and Environmental Science* 4 (2011) 1372–1378.
- [49] S. Shen, L. Guo, X. Chen, F. Ren, S.S. Mao, Effect of Ag₂S on solar-driven photocatalytic hydrogen evolution of nanostructured CdS, *International Journal of Hydrogen Energy* 35 (2010) 7110–7115.
- [50] S. Shen, X. Chen, F. Ren, C.X. Kronawitter, S.S. Mao, L. Guo, Solar light-driven photocatalytic hydrogen evolution over ZnIn₂S₄ loaded with transition-metal sulfides, *Nanoscale Research Letters* 6 (2011) 290.
- [51] P.F. Liu, J.K. Chu, S.J. Hou, P. Xu, J.Y. Zheng, Numerical simulation and optimal design for composite high-pressure hydrogen storage vessel: a review, *Renewable and Sustainable Energy Reviews* 16 (2012) 1817–1827.
- [52] D. Hanane, Models, methods and approaches for the planning and design of the future hydrogen supply chain, *International Journal of Hydrogen Energy* 37 (2012) 5318–5327.
- [53] T. Abbasi, S.A. Abbasi, ‘Renewable’ hydrogen: prospects and challenges, *Renewable and Sustainable Energy Reviews* 15 (2011) 3034–3040.
- [54] G.E. Froudakis, Hydrogen storage in nanotubes & nanostructures, *Materials Today* 14 (2011) 324–328.
- [55] F. Ding, B.I. Yakobson, Challenges in hydrogen adsorptions: from physisorption to chemisorption, *Frontiers of Physics* 6 (2011) 142–150.
- [56] B. Sakintuna, F. Lamari-Darkrim, M. Hirscher, Metal hydride materials for solid hydrogen storage: a review, *International Journal of Hydrogen Energy* 32 (2007) 1121–1140.
- [57] S. Bouaricha, J.P. Dodeley, D. Guay, J. Huot, S. Boily, R. Schulz, Hydriding behavior of Mg–Al and leached Mg–Al compounds prepared by high-energy ball-milling, *Journal of Alloys and Compounds* 297 (2000) 282–293.
- [58] T. Hirata, T. Matsumoto, M. Amano, Y. Sasaki, Dehydriding reaction kinetics in the improved intermetallic Mg₂Ni–H system, *Journal of the Less Common Metals* 89 (1983) 85–91.
- [59] S. Barcelo, M. Rogers, C.P. Grigoropoulos, S.S. Mao, Hydrogen storage property of sandwiched magnesium hydride nanoparticle thin film, *International Journal of Hydrogen Energy* 35 (2010) 7232–7235.
- [60] M. Rogers, S. Barcelo, X. Chen, T.J. Richardson, V. Berube, G. Chen, M.S. Dresselhaus, C.P. Grigoropoulos, S.S. Mao, Hydrogen storage characteristics of nanograined free-standing magnesium–nickel films, *Applied Physics A* 96 (2009) 349–352.
- [61] S. Barcelo, S.S. Mao, High throughput optical characterization of alloy hydrogenation, *International Journal of Hydrogen Energy* 35 (2010) 7228–7231.
- [62] L.J. Murray, M. Dincă, J.R. Long, Hydrogen storage in metal–organic frameworks, *Chemical Society Reviews* 38 (2009) 1294–1314.
- [63] A. Hunt, *Encyclopedia Britannica Science Year Book*, 1996, p. 146.
- [64] S.S. Mao, K.R. Carrington, X. Chen, A. Hunt, K. Gross, Hydrogen storage in ultra-low density silica aerogel, private communication.
- [65] A.J. Hunt, K. Gross, S.S. Mao, Mesoporous oxides and their applications to hydrogen storage, *Materials Matter* 4 (2009) 47–52.
- [66] W. Yuan, Y. Tang, X. Yang, Z. Wan, Porous metal materials for polymer electrolyte membrane fuel cells—a review, *Applied Energy* 94 (2012) 309–329.
- [67] S. Barceló, S.S. Mao, Hydrogen fuel cell technology and its potential for aviation, *Professional Pilot Magazine* 44 (2010) 70.
- [68] S. Sharma, B.G. Pollet, Support materials for PEMFC and DMFC electrocatalysts—a review, *Journal of Power Sources* 208 (2012) 96–119.
- [69] H.A. Gasteiger, S.S. Kocha, B. Sompalli, F.T. Wagner, *Applied Catalysis B* 56 (2005) 9–35.
- [70] W. Chrzanowski, A. Wieckowski, Surface structure effects in platinum/ruthenium methanol oxidation electrocatalysis, *Langmuir* 14 (1998) 1967–1970.

- [71] R. Othman, A.L. Dicks, Z. Zhu, Non precious metal catalysts for the PEM fuel cell cathode, *International Journal of Hydrogen Energy* 37 (2012) 357–372.
- [72] J.M. Lackner, W. Waldhauser, B. Major, J. Morgiel, L. Major, H. Takahashi, T. Shibayam, Growth structure and growth defects in pulsed laser deposited Cr–CrN_x–CrC_xN_{1-x} multilayer coatings, *Surface and Coatings Technology* 200 (2006) 3644–3649.
- [73] K. Volz, M. Kiuchi, W. Ensinger, Structural investigations of chromium nitride films formed by ion beam-assisted deposition, *Surface and Coatings Technology* 108 (1998) 303–307.
- [74] H. Zhong, X. Chen, H. Zhang, M. Wang, S.S. Mao, Proton exchange membrane fuel cells with chromium nitride nanocrystals as electrocatalysts, *Applied Physics Letters* 91 (2007) 163103.



Samuel Mao is Director of Clean Energy Engineering Center at the University of California at Berkeley. He received his Ph.D. degree from Berkeley in 2000, and since then he has been leading a multidisciplinary research team developing clean energy technologies as well as investigating enabling materials science. He has published over a hundred peer-reviewed journal articles, which

have received more than 10,000 citations. He has served as a technical committee member, program review panelist, grant proposal reviewer, and national laboratory observer for the U.S. Department of Energy. He was a founding co-chair/organizer of the *1st International Conference on Energy Nanotechnology*, the *1st International Symposium on Transparent Conducting Materials*, and the *1st International Workshop on Renewable Energy*. He was a general chair for the 2011 Spring *Materials Research Society (MRS) Meeting*, and co-chaired the 2012 *International Conference on Clean Energy*. He is the recipient of a 2011 “R&D 100” Technology Award.